Structural and Capacitive Properties of Graphene Obtained by a Green Method of Graphene Oxide Reduction

M. Raić, D. Sačer, and M. Kraljić Roković*
Faculty of Chemical Engineering and Technology,
University of Zagreb, Marulićev trg 19,
10000 Zagreb, Croatia

https://doi.org/10.15255/CABEQ.2019.1609

Original scientific paper
Received: January 29, 2019
Accepted: September 11, 2019

In this study, a green method was applied in order to reduce graphene oxide (GO). Reduction was carried out at 80 °C in the presence of phenolic compounds from olive leaf extract (OLE), and olive mill wastewater (OMW) as a reducing agent. Owning to the natural origin of the reducing agent, this method is environmentally friendly. Reduction was carried out at pH=7 and pH=10 in the presence of OLE, and at pH=10 in the presence of OMW. The reduction process was monitored using UV/Vis spectroscopy. The structural properties of the reduced graphene oxide (rGO) samples were characterized by Fourier-transform infrared spectroscopy (FTIR) and thermogravimetric analysis (TGA). Structural studies demonstrated that a part of the oxygen functionalities in the graphene oxide structure had been removed, which resulted in increased electrical conductivity as proved by the four-point probe method. Better reduction efficiency, as well as better capacitive properties, were obtained at increased pH value. Capacitive properties of rGO were determined using the cyclic voltammetry technique. The influence of the different reducing agents, OLE and OMW, on rGO capacitive properties is also shown in this work.

Keywords:
graphene, graphene oxide, capacitive properties, olive leaf extract, olive mill wastewater

Introduction

Graphene[1] is a two-dimensional nanostructure with single-layer carbon atoms firmly packed into a honeycomb crystal lattice.[2] Such a structure results in unique mechanical, thermal, catalytic, electrical, and optical properties, and has attracted tremendous attention in recent years. Graphene holds the potential to be used in a wide range of fields, such as bio-sensing, drug delivery, catalysis, and energy storage.[3] Supercapacitors based on graphene are promising alternatives for battery systems, owing to a large surface area of graphene and high electronic conductivity. These properties enable high power and energy densities of the supercapacitor.[4–9]

At present, graphene is being prepared by various techniques, such as micromechanical cleavage, epitaxial growth, chemical vapor deposition, electric arc discharge, ultrasonic synthesis, chemical reduction of graphene oxide, and spray pyrolysis.[10] In general, the production of individual graphene sheets in bulk quantity proves to be a significant challenge, which can be solved by the chemical reduction of graphene oxide (GO).[3] So far, strong chemical reductants, such as hydrazine (N_2H_4), thermal reduction, hydrothermal synthesis, microwave irradiation or electrochemical reduction have been utilized for reducing the chemically exfoliated GO sheets.[11–13] Recently, there have been reports on green reduction routes which use reducing agents such as ascorbic acid,[14–16] green tea,[17] reducing sugar,[18] baker's yeast[19] or amino acids.[16,20]

In this article, we demonstrate a simple and green chemistry route for the preparation of reduced graphene oxide (rGO) through the reduction of GO using olive leaf extract (OLE) or olive mill wastewater (OMW). Olives and olive-derived products are known as a valuable source of natural phenolic compounds that exhibit antioxidant properties. The strongest antioxidant activity was noted for hydroxytyrosol, oleuropein, pinoresinol, ligstroside, and tyrosol.[21] High amounts of OMW are generated in the Mediterranean area during the olive oil production processes,[22] and therefore OMW can be used as an economically and ecologically sustainable and cheap reducing agent.

The goal of this work was to use OLE as a commercially controlled product and OMW as purified wastewater released from olive fruit during the

*Corresponding author: E-mail: mkralj@fkit.hr,
phone: +385 1 4597112, fax: +385 1 4597130

oil production process. According to authors knowledge, there is only one report where the effect of OLE on the reduction of GO has been reported.[23] The reduction process was monitored using UV/Vis spectroscopy, while the characterization of rGO was carried out by FTIR, thermogravimetric analysis (TGA), and four-point probe (FPP). Capacitive properties of rGO were determined using the cyclic voltammetry (CV) method.

Experimental procedure

Preparation of reduced graphene oxide

Graphite oxide was prepared and purified according to Hoffmann´s method.[24] Nitric acid, 9 mL (65 %) and sulfuric acid 17.5 mL (95 – 98 %) were added and mixed in a reaction flask using a magnetic stirring bar. The reaction flask containing the mixture was added into an ice bath and cooled down to temperatures between 0 – 5 °C. Graphite, 1 g (natural flakes, Sigma Aldrich, USA) was then added to the mixture under vigorous stirring to obtain homogeneous dispersion. Reaction flask was kept at temperatures lower than 5 °C in the ice bath. Next, potassium chlorate (11 g) was slowly added to the mixture over a period of 30 minutes to avoid increase in temperature.

After complete dissolution of the potassium chlorate, the mixture was vigorously stirred for 96 hours at room temperature. The product of oxidation, graphite oxide, was then poured into redistilled water (1000 mL), filtered, redispersed, and washed repeatedly with HCl solution (5 %) and with redistilled water until a neutral pH of the filtrate was obtained.

Graphene oxide (GO) suspension was obtained by ultrasonication of the graphite oxide in deionized water (40 kHz) for 2 hours, and centrifuged at 4000 rpm to remove any non-exfoliated graphite or graphite oxide particles. Mass concentration of obtained suspension was 8.56 mg mL^{-1}. To remove any other impurities and residual ions from oxidation step, GO suspension was dialyzed for one week in redistilled water using Spectra/Por 4 dialysis tubing.

The chemical reduction of GO was carried out with two different reducing agents, olive leaf extract (OLE, Magdis d.o.o.) at two different pH values (7 and 10), and olive mill wastewater (OMW, oil production plant "Lucija", island of Pašman, 2015.) at pH value 10. In a procedure for chemical conversion of GO to graphene, 34 mL of graphene oxide solution was diluted with 256 mL of OLE or OMW solution to obtain mass concentration of GO 1 mg mL^{-1} and mass concentration of phenolic compounds 4 mg mL^{-1}. The mass concentration of the phenolic compounds was determined using UV/Vis spectroscopy and calibration curve of caffeic acid. The mixture was heated at 80 °C during 5 hours with stirring.

After the reduction process, the reduced graphene oxide (rGO) was filtered and intensively washed with redistilled water and ethanol. The rGO obtained using OLE at pH=7 was denoted as rGO(OLE, pH=7), rGO obtained using OLE at pH=10 was denoted rGO(OLE, pH=10), and rGO obtained using OMW at pH=10 was denoted rGO(OMW, pH=10). After synthesis, the samples were oven-dried for 24 hours at 60 °C. The rGO suspension was filtered under vacuum through a propylene cellulose filter and then air-dried. Separation from the filter membrane yielded approximately 1 mm thick rGO papers.

The reduction reaction was monitored by recording the UV/Vis absorption spectra of reaction mixture as a function of time. Ocean Optics 200 with the radiation source Model D 1000 CE, Analytical Instrument Systems Inc., USA was used.

Materials characterization

FTIR spectroscopy was applied to identify the characteristic peaks of oxygen-containing groups in GO and rGO samples. FTIR spectra were recorded using a Perkin Elmer Instruments, Spectrum One. The thermal stability of the rGO samples was determined by thermogravimetric analysis (TGA) using TA Instruments Q500. The mass of the samples was 8 to 10 mg. The measurement was conducted in a nitrogen stream at a flow rate of 60 mL min^{-1} at heating rate of 10 °C min^{-1} in the temperature range from 25 °C to 700 °C.

Electrical resistance of rGO paper was measured using Keysight 34461A instrument and four-point probe method.

Electrical conductivity was determined according to equations 1 and 2:

$$\rho = \frac{\pi \cdot d \cdot R}{\ln 2} \tag{1}$$

$$\kappa = \frac{1}{\rho} \tag{2}$$

where ρ is resistivity (Ω cm), R is resistance (Ω), d is thickness of the sample (m), and κ conductivity (S cm^{-1}).

Electrochemical characterization

Electrochemical properties were determined by cyclic voltammetry method. Three-electrode system was connected to the EG&G Princeton Applied Re-

search, model 273A potentiostat. A working electrode was glassy carbon (GC) disc coated with rGO active material. In order to prepare working electrode, 2.5 μL of rGO/NMP suspension (10 mg mL^{-1}) was drop-casted on clean GC disc electrode (A=0.07 cm^2), and dried at room temperature for 24 hours. Saturated calomel electrode was used as a reference electrode and Pt foil (A=0.5 cm^2) as counter electrode. The electrodes were tested in 0.5 mmol mL^{-1} Na_2SO_4 aqueous solution. The total amount of stored charge or the value of electrode specific capacitance was calculated according to equation 3:

$$C_s = \frac{\int_{E_1}^{E_2} I(E)\mathrm{d}E}{2mv(E_1 - E_2)} \quad (3)$$

where C_s is the specific capacitance (F g^{-1}), I is the current, A, E_1 is the initial potential (V), E_2 is the final potential (V), v is the scan rate (V s^{-1}), m is the mass of rGO (g).

The solutions of OLE and OMW in phosphate buffer of pH=5.5 were tested by cycling voltammetry method and three-electrode system. The concentration of phenolic compounds in OLE and OMW was 4 mg mL^{-1}. The pH value of the buffer solution corresponded to pH value of Na_2SO_4 solution. The working electrode was GC. Prior to measurement, the surface of the GC electrode was polished on 0.05 mm alumina powder and activated by performing 10 cycles in phosphate buffer of pH=7 within potential range –1 V and 1.5 V at scan rate of 50 mV s^{-1}.[25]

Results and discussion

UV/Vis spectrophotometry

UV/Vis spectroscopy was used to monitor the GO reduction, at elevated temperature in the presence of phenolic compound from OLE and OMW, as a function of time. UV/Vis spectrum (Fig. 1a,b) shows the absorption maximum at about 230–250 nm corresponding to π-π* transitions of sp2 hybridized carbon atoms within the graphene oxide structure. The other absorption maximum appears at about 270–300 nm, and corresponds to n–π* transition characteristic for oxygen functionalities. It is well known that π-π* transition peak moves to higher wavelengths when GO is transformed to rGO.[17] However, in our case, such an effect was not obtained, but it was noted that the intensity of absorbance had changed upon reduction. The absorbance spectrum of OLE is similar to GO because it contains phenolic compounds[26,27] that include aromatic structure and hydroxyl groups. However, the intensity and peak position in absorbance spectra is

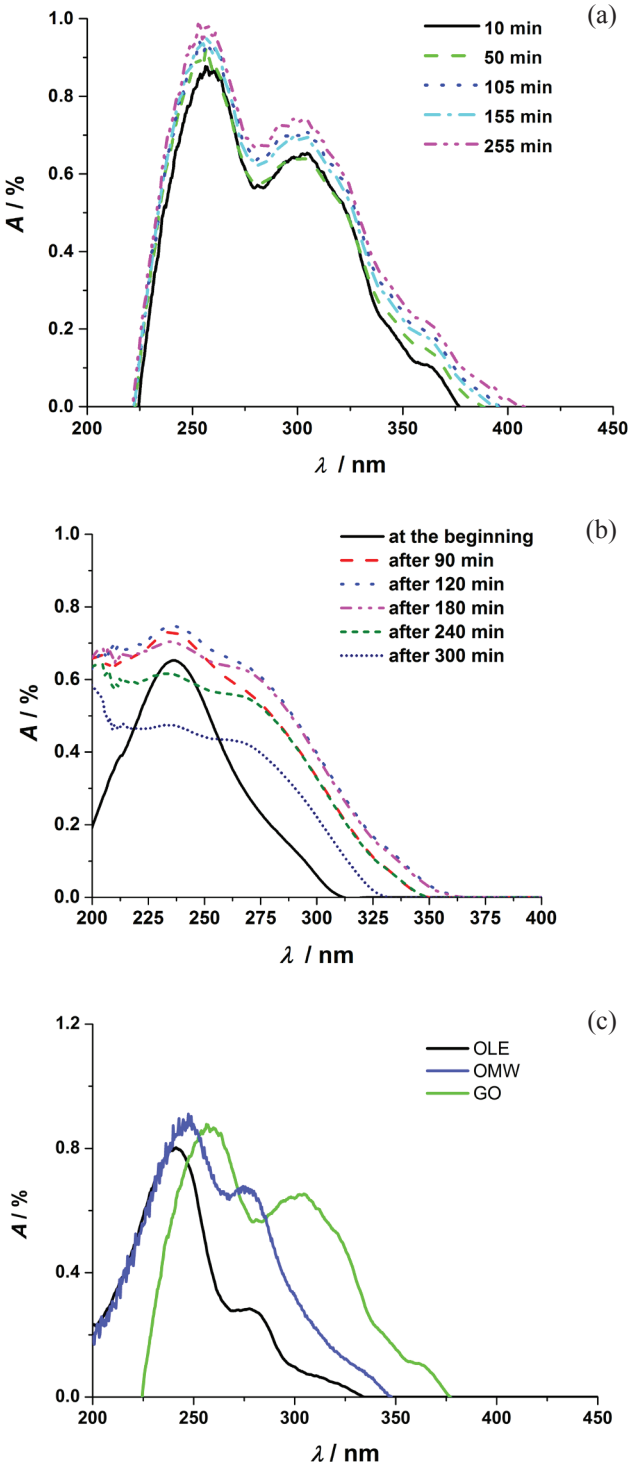

Fig. 1 – *UV/Vis spectrum recorded a) during thermal treatment of GO, and b) during thermal treatment of GO in the presence of OLE at pH=10. c) Comparison of UV/Vis spectrum recorded for pure GO, OLE and OMW.*

not the same (Fig. 1c). Therefore, the absorbance in the case of solution containing OLE and GO is a result of overlapping peaks corresponding to OLE and GO. Fig. 1b reflects properties of the mixture at different times during the reduction process. In the case of GO without OLE, the intensity gradually in-

creased up to 255 min (Fig. 1a). On the other hand, in the presence of OLE, the intensity increased up to 120 min, after which it started to decrease (Fig. 1b). From the obtained results, two important conclusions can be drawn. Firstly, during the reduction process, transformation of dissolved GO into small insoluble particles of rGO takes place, and therefore light scattering in a wide wavelength range appears, rather than light transmittance through the sample. The light scattering increases the absorption peak intensity. The intensity increase in whole spectral region during successful reduction process was noticed previously, and it was attributed to gas evolution and the regeneration of sp2 bonds.[28–30] Secondly, the intensity change is more pronounced in the presence of OLE, which indicates its good efficiency as a reducing agent. It was also noticed that, after appropriate reduction time, in the presence of OLE, absorption intensity decreased again. This effect is most likely obtained owing to the further agglomeration of rGO that results in decreased light scattering or owing to the significant decrease in GO concentration. From the obtained results, it seems that, although the reduction process was in progress, as the mixture evidently changed in color from brown to black,, the redshift of peak at 230 nm was not obtained. However, the absorption intensity change noticed in this work indicated that reduction took place. Additionally, the difference obtained in the presence and absence of OLE, points out that this process is more progressive in the presence of OLE.

UV/Vis spectroscopy was also used to compare solutions containing OLE and OMW (Fig. 1c). It is obvious that intensity of absorbance at 280 nm is more pronounced for OMW; therefore, different composition of the phenolic compounds in these two solutions was expected.

FTIR analysis

FTIR spectrum corresponding to GO (Fig. 2a) shows broad absorption band in the 3600–2500 cm^{-1} region assigned to –OH stretching mode of mostly water incorporated within GO structure, but it also indicates alkoxy groups that are incorporated within the graphene structure. Characteristic absorption band for GO at 1715 cm^{-1} was assigned to carbonyl group originating from carboxyl, aldehydes or ketones. The band at 1616 cm^{-1} can be assigned to one of the following: asymmetric C=C stretching or –OH bending modes, and water physisorbed on the GO.[15] Additional band ascribed to –OH deformation was registered at 1379 cm^{-1}, whilst absorption bands at 1237 cm^{-1} and 1052 cm^{-1} were commonly assigned to epoxy and alkoxy C–O stretching vibrations, respectively.

After the reduction process, the band at 1616 cm^{-1} shifts to 1638 cm^{-1} while band at 1715 cm^{-1} shifts in the range between 1700–1730 cm^{-1}. In the case of rGO(OLE pH=10) and rGO(OLE pH=7) these band partially overlap, and therefore it was hard to distinguish the band maximum. However, partial GO reduction was confirmed by changing the band position and decreasing the ratio between intensity of peak at 1638 cm^{-1} and peak at 1720–1730 cm^{-1}. The absorption spectrum of rGO samples shows additional peak that is not recorded for GO at 1536 cm^{-1} for rGO(OMW pH=10), at 1544 cm^{-1} for rGO(OLE pH=10) and at 1540 cm^{-1} for rGO(OLE pH=7) that corresponds to aromatic in plane skeletal vibration.[31,32] The rGO spectrum peaks in the region 1180–1440 cm^{-1} [33] were less pronounced compared to the wide band obtained for GO. The resulting FTIR spectrum shows that the rGO(OMW pH=10) sample contains phenolic compounds as it is evident by bands at 2852 cm^{-1} and 2918 cm^{-1} that were also observed in the spectrum of OLE or OMW sample (Fig. 2b). This band is characteristic for aliphatic C–H stretching vibrations[34,35]. In the case of rGO(OLE), there were no typical peaks for OLE at 2852 cm^{-1} and 2953 cm^{-1}, therefore it can be concluded that, after reduction, OLE was completely removed from the sample by washing.

Finally, it can be concluded that phenolic compounds cannot entirely remove GO oxygen functional groups,[31,36–39] which was further confirmed with TGA analysis (Fig. 2).

TGA analysis

Thermal stability was used to assess the reduction degree of rGO samples, since it is well known that the amount of oxygen decreases by increasing the degree of reduction due to CO_2 formation. From Fig. 3, it is evident that all samples exhibit a loss of absorbed water molecules around 100 °C. The degradation of oxygenated functional groups starts above 100 °C with significant weight loss between 250 – 300 °C. Fig. 3 shows that a total weight loss at 700 °C was 45 – 55 %, depending on the sample. The result indicated that the greatest mass loss was obtained for rGO(OLE, pH=7). Therefore, it can be concluded that the process of removing oxygen functional groups is more effective at higher pH values. The results are also in agreement with the previous studies suggesting that the reduction of GO is pH-dependent.[12] However, the impact of pH on the activity of phenolic compound should also be taken into account as it is well known that oxidation potential of phenolic compounds decreases with a pH increase, and thus, higher reduction activity of OLE is expected at elevated pH value.[40]

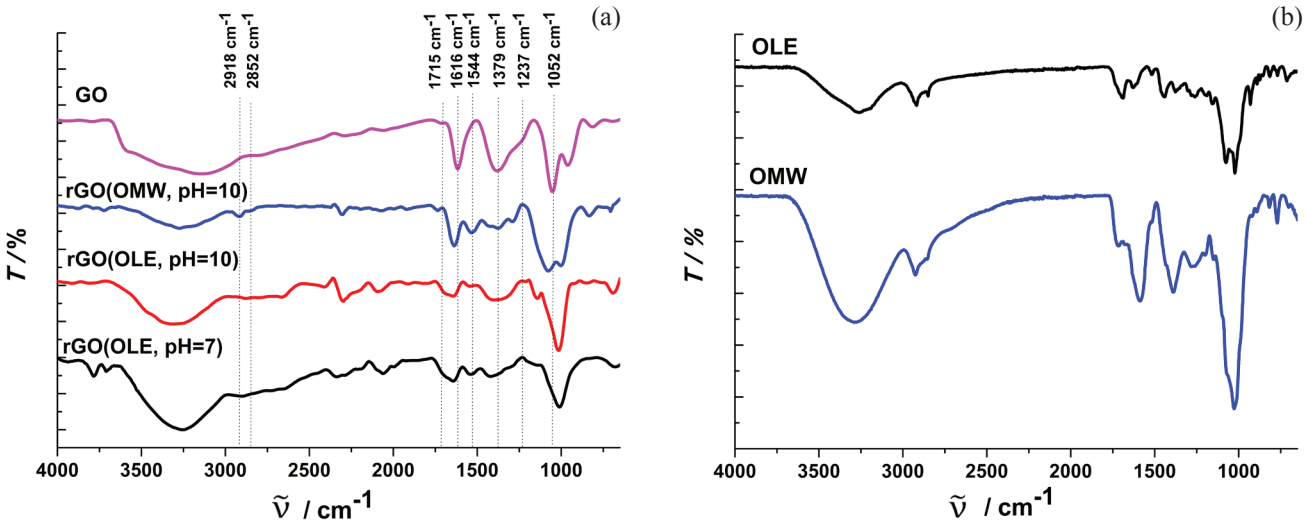

Fig. 2 – *FTIR spectra of a) GO and rGO samples, and b) OLE and OMW samples*

Four-point probe

Electrical conductivity measurements were carried out in order to confirm that the GO reduction process was conducted successfully. For this purpose, the four-point probe method was used.

GO shows lower conductivity than that of pristine graphite or rGO owning to the fact that sp2 bonds have been disrupted during oxidation. The regeneration of sp2 bonds and conductivity increase is achieved by the reduction process. The conductivity values obtained in this work, (Table 1), are significantly higher compared to the value previously reported for GO ($6.8 \cdot 10^{-10}$ S cm^{-1}),[41] which is a good indication of successful reduction. By comparing the rGO conductivity in this work with the values previously reported for rGO, it can be concluded that the obtained values are within the range that was previously reported.[41,42] Additionally, higher conductivity was obtained for the rGO(OLE) prepared at higher pH values, which supports previous conclusions related to reduction efficiency and pH value. The conductivity obtained for rGO(OMW, pH=10) deviated from the values obtained for rGO(OLE), i.e., higher conductivity was registered. However, the TGA result indicated no lower content of oxygen for rGO(OMW, pH=10) sample as it would be expected for higher conductivity (Fig. 3). The only explanation for this behavior could be that the mass decrease recorded for rGO(OMW, pH=10) included degradation of phenolic compounds that were evidently present within this sample. Therefore, greater mass change was registered for rGO(OMW, pH=10) that would be obtained for rGO with the same degree of reduction but without phenolic compounds. From the obtained conductivity, it follows that the slightly higher degree of sp2 bond regeneration was achieved for the sample prepared in the presence of OMW.

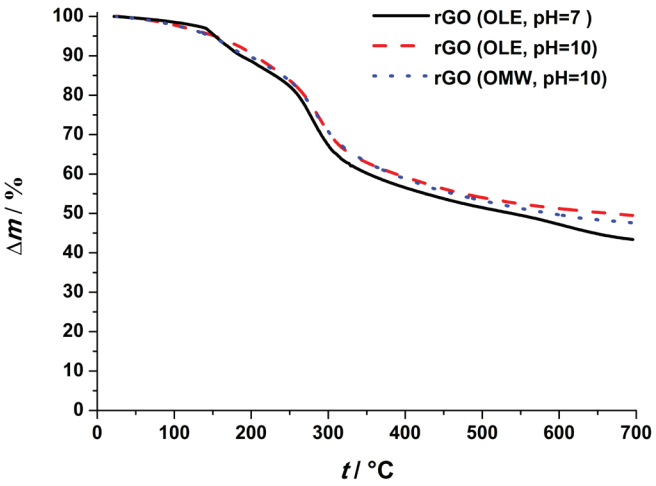

Fig. 3 – *Thermogravimetry analysis of rGO samples*

Table 1 – *Resistance and electrical conductivity values for the different rGO thin films*

Sample	R/Ω	d/μm	κ/S cm^{-1}
rGO(OLE, pH=7)	3050	0.60	1.206
rGO(OLE, pH=10)	1270	0.33	5.265
rGO(OMW, pH=10)	247	0.58	15.403

Electrochemical characteristics

From the cyclic voltammetry responses (Fig. 4), it can be concluded that, for all the electrodes containing rGO, high currents within the wide potential range were registered, indicating good capacitive behavior. Such a property opens up the possibility of using these materials in supercapacitor.[4–9] Higher current values that were obtained for the rGO electrodes, compared to the GO electrode, indicated that GO was successfully reduced. The reduction process resulted in sp2 bond regeneration,

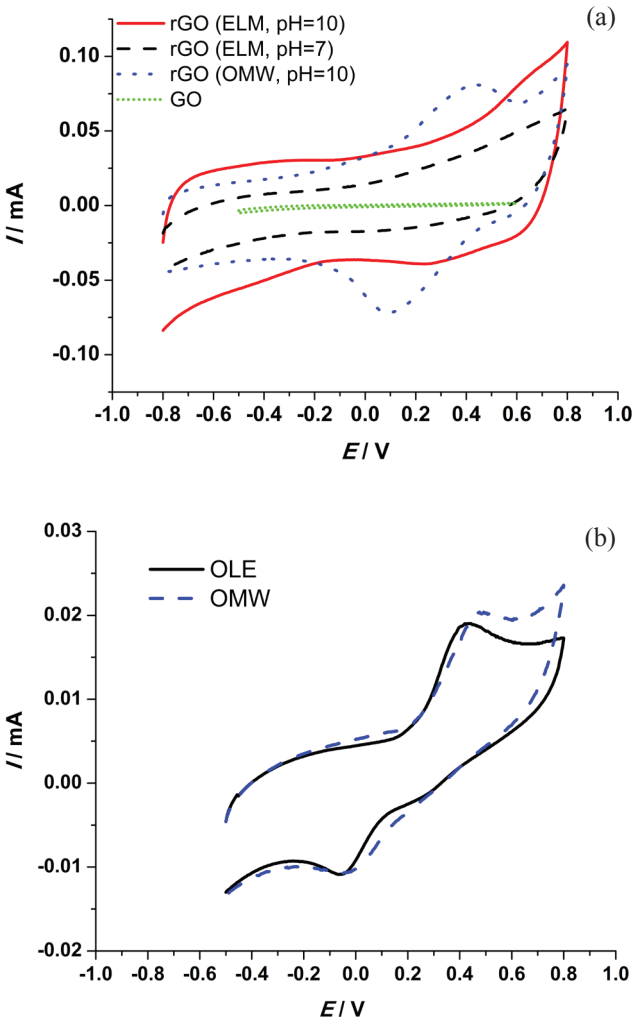

Fig. 4 – *Cyclic voltammograms for a) different rGO electrodes in 0.5 mol dm^{-3} Na_2SO_4, and b) GC electrode in OLE and OMW buffer solutions of pH=5.5, v=50 mV s^{-1}*

Table 2 – *Specific capacitance values for different rGO electrodes*

Sample	C_s/F g^{-1}
rGO(OLE, pH=7)	16.6
rGO(OLE, pH=10)	34.0
rGO(OMW, pH=10)	32.3

reduction in oxygen functionalities, and increase in conductivity (Fig. 5). The increased conductivity enables double-layer charging/discharging on the rGO surface, which governs the capacitive behavior of the material. An additional current peak was recorded in the cyclic voltammogram for the rGO(OMW, pH=10) electrode in the potential range from 100 mV to 500 mV. It can be assumed that this peak corresponds to the redox reaction of the residual phenolic compounds positioned on the top of rGO sheets. In order to prove such an assumption, OLE and OMW solutions were tested using GC electrode and cyclic voltammetry method (Fig. 4b). As a result of phenolic compound redox reaction, anodic and cathodic current peaks were registered. The obtained behavior was similar to the response of rGO(OMW, pH=10), which confirmed the previous assumption that phenolic compounds influence cyclic voltammetry response. Additionally, the peak potentials for the two different solutions differed insignificantly, indicating similar antioxidant activity of phenolic compounds present in OLE and OMW.[40]

Fig. 4a also shows that the highest capacitive current was registered for rGO(OLE, pH=10), so it could be concluded that the highest degree of re-

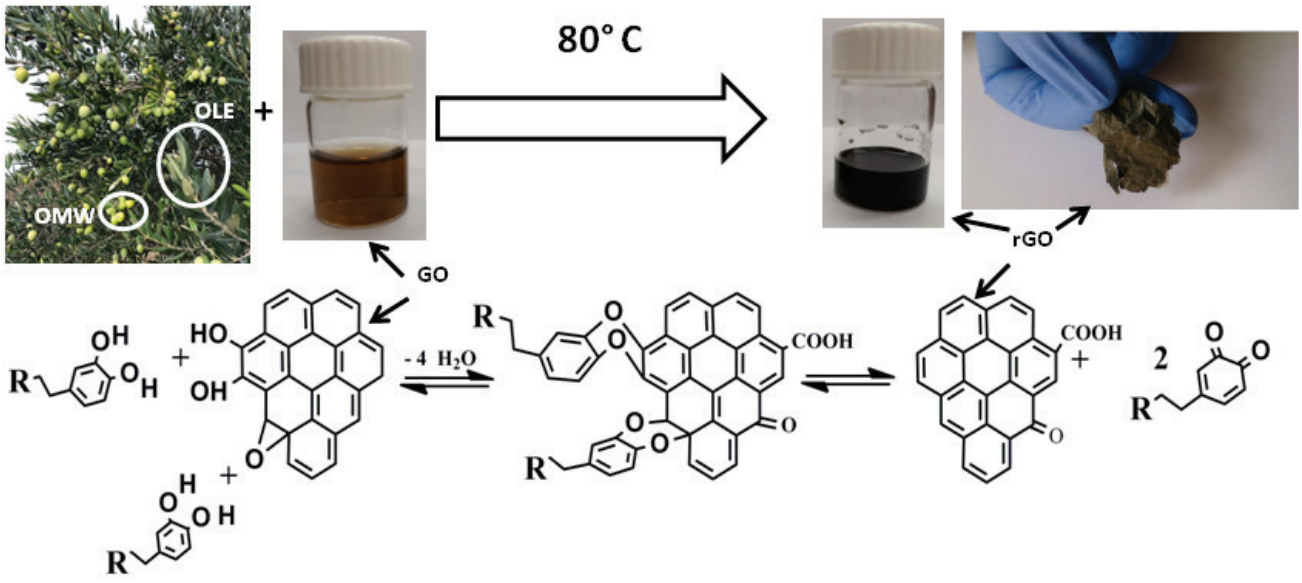

Fig. 5 – *Schematic representation of the reduction process, reactants, and obtained products*

duction was achieved for this sample. The values obtained for conductivity point to the opposite conclusion, since the highest conductivity was registered for rGO(OMW, pH=10). Therefore, it is obvious that the presence of phenolic compounds reduced the capacitive currents of rGO(OMW, pH=10).

From the cyclic voltammogram, it is possible to determine the total amount of stored charge or the value of electrode specific capacitance (Table 2) according to equation (3). The highest value of specific capacitance was obtained for the rGO(OLE, pH=10) electrode, 34.0 F g^{-1}, and a similar value was obtained for the rGO(OMW, pH=10) electrode, 32.3 F g^{-1}. Although the cyclic voltammogram for rGO(OMW, pH=10) showed lower capacitive current in the wide potential range, compared to rGO(OLE, pH=10), the similar capacitance was calculated for both layers owning to the contribution of current peak to overall charge. Since the current peak was not completely reversible, which is a necessary condition for good pseudocapacitive behavior, it followed that rGO(OLE, pH=10) showed better capacitive properties. Please note that nearly half of this value was obtained for the rGO(OLE, pH=7) electrode, 16.6 F g^{-1}, which was additional confirmation for the lower degree of reduction at lower pH value. The results obtained in this work are comparable with the specific capacitance values reported previously, which were mostly within the range of 25–200 F g^{-1}.[4,43–46] Successful reduction of GO in the presence of OLE and OMW at elevated temperature opens up the possibility of applying it as a reducing agent even in other synthesis methods that result in more porous material and significantly greater specific capacitance values.

Conclusions

The reduction of GO to rGO was carried out successfully using OLE and OMW as environmentally friendly reducing agents. In this process, a significant reduction in oxygen functional groups and regeneration of sp2 hybridization was achieved, which was proven using FTIR, TGA, and by measuring the electrical conductivity of the prepared samples.

Thermogravimetric analysis indicated that the highest reduction efficiency was obtained for the rGO(OLE, pH=10) sample, whereas the lowest efficiency was obtained for rGO(OLE, pH=7). The electrical conductivity measurements indicated a similar trend if taking into account the influence of pH value. However, the highest conductivity was recorded for rGO(OMW, pH=10). FTIR method indicated that the reduction process induced regeneration of sp2 bonds, but without the complete removal of oxygen functional groups.

Good capacitive behavior of all rGO electrodes was confirmed using the cyclic voltammetry method. The obtained results indicated that better capacitive properties had been obtained for rGO(OLE, pH=10), 34.0 F g^{-1}, compared to rGO(OLE, pH=7), 16.6 F g^{-1}. Taking into account the various reducing agents, it was evident that, although somewhat higher conductivity was registered for rGO(OMW, pH=10), better capacitive properties were obtained for the rGO (OLE, pH=10) electrode. The cyclic voltammetry and FTIR spectroscopy methods revealed the presence of phenolic compounds within the rGO(OMW, pH=10) sample. On the other hand, such an effect was not registered for rGO(OLE) samples. Based on the reported results, it was concluded that the phenolic compounds present within rGO(OMW, pH=10) sample had a significant impact on rGO capacitive properties.

List of symbols

A – absorbance, %
A – surface, m^2
C_s – specific capacitance, F g^{-1}
d – thickness, m
E_1 – initial potential, V
E_2 – final potential, V
E – potential, V
f – frequency, Hz
I – current, A
m – mass, g
R – resistance, Ω
T – transmittance, %
t – temperature, °C
κ – conductivity, S cm^{-1}
λ – wavelength, nm
ρ – resistivity, Ω cm
Δm – mass change, g
γ – mass concentration, g L^{-1}
ν – scan rate, V s^{-1}
$\tilde{\nu}$ – wavenumber, cm^{-1}

Abbreviations

CV – cyclic voltammetry
FPP – four point probe
FTIR – Fourier-transform infrared spectroscopy
GO – graphene oxide
NMP – N-methyl-2-pyrrolidone
OLE – olive leaf extract

OMW – olive mill wastewater
rGO(OLE, pH=10) – rGO obtained using OLE at pH=10
rGO(OLE, pH=7) – rGO obtained using OLE at pH=7
rGO(OMW, pH=10) – rGO obtained using OMW at pH=10
rGO – reduced graphene oxide
rpm – revolutions per minute
TGA – thermogravimetric analysis
UV/Vis – ultraviolet-visible spectroscopy

ACKNOWLEDGEMENT

This work has been fully supported by the Croatian Science Foundation under the project ″High power-high energy electrochemical supercapacitor for hybrid electrical vehicles″, IP-2013-11-8825.

The authors thank Magdis d. o. o. for providing us the olive leaf extract used in this work, oil production plant "Lucija" for providing us the olive mill wastewater and Denis Paleka for providing us the olive tree photography.

References

1. *Geim, A. K., Novoselov, K. S.*, The rise of graphene, Nat. Mater. **6** (2007) 183. doi: https://doi.org/10.1142/9789814287005_0002
2. *Allen, M. J., Tung V. C., Kaner, R. B.*, Honeycomb carbon: A review of graphene, Chem. Rev. **110** (2010) 132. doi: https://doi.org/10.1021/cr900070d
3. *Sadhukhan, S., Ghosh, T. K., Rana, D., Roy, I., Bhattacharyya, A., Sarkar, G., Chakraborty M., Chattopadhyay, D.,* Studies on synthesis of reduced graphene oxide (RGO) via green route and its electrical property, Mater. Res. Bull. **79** (2016) 41. doi: https://doi.org/10.1364/OE.25.005415
4. *Yang, X., Zhu, J., Qiu, L., Li, D.,* Bioinspired effective prevention of restacking in multilayered graphene films: Towards the next generation of high-performance supercapacitors, Adv. Mater. **23** (2011) 2833. doi: https://doi.org/10.1002/adma.201100261
5. *Yang, X., Cheng, C., Wang, Y., Qiu, L., Li D.*, Liquid-mediated dense integration of graphene materials for compact capacitive energy storage, Science **80** (2013) 534. doi: https://doi.org/10.1126/science.1239089
6. *Sačer, D., Kralj, M., Sopčić, S., Košević, M., Dekanski, A., Kraljić Roković, M.*, Supercapacitors based on graphene/pseudocapacitive materials, J. Serb. Chem. Soc. **82** (2017) 411. doi: https://doi.org/10.2298/JSC170207027S
7. *Hantel, M. M., Kaspar, T., Nesper, R., Wokanu, A., Kötz, R.,* Partially reduced graphene oxide paper: A thin film electrode for electrochemical capacitors, J. Electrochem. Soc. **160** (2013) 747. doi: https://doi.org/10.1149/2.019306jes
8. *Nardecchia, S., Carriazo, D., Ferrer, M. L., Gutiérrez, M., del Monte, F.,* Three dimensional macroporous architectures and aerogels built of carbon nanotubes and/or graphene: Synthesis and applications, Chem. Soc. Rev. **42** (2013) 794. doi: https://doi.org/10.1039/C2CS35353A
9. *Sačer, D., Spajić, I., Kraljić Roković, M., Mandić, Z.*, New insights into chemical and electrochemical functionalization of graphene oxide electrodes by o-phenylenediamine and their potential applications, J. Mater. Sci. **53** (2018) 15285. doi: https://doi.org/10.1007/s10853-018-2693-6
10. *Illakkiya, T. J., Rajalakshmi, U. P., Oommen, R.,* Nebulized spray pyrolysis: A new method for synthesis of graphene film and their characteristics, Surf. Coat. Tech. **307** (2016) 65. doi: https://doi.org/10.1016/j.surfcoat.2016.08.051
11. *Akhavan, O., Kalaee, M., Alavi, Z. S., Ghiasi, S. M. A, Esfandiar A.,* Increasing the antioxidant activity of green tea polyphenols in the presence of iron for the reduction of graphene oxide, Carbon **50** (2012) 3015. doi: https://doi.org/10.1016/j.carbon.2012.02.087
12. *Tai, G., Zeng, T., Li, H., Liu, J., Jizhou, K., Fuyong, L.,* Temperature and pH effect on reduction of graphene oxides in aqueous solution, Mater Res. Express **1** (2014) 35605. doi: https://doi.org/10.1088/2053-1591/1/3/035605
13. *Karačić, D., Korać, S., Dobrota, A. S., Pašti, I., Skorodumova, N. V., Gutić, S.,* When supporting electrolyte matters – Tuning capacitive response of graphene oxide *via* electrochemical reduction in alkali and alkaline earth metal chlorides, Electrochim. Acta **297** (2019) 112. doi: https://doi.org/10.1016/j.electacta.2018.11.173
14. *Zhang, J., Yang, H., Shen, G., Cheng, P., Zhang, J., Guo, S.,* Reduction of graphene oxide via L-ascorbic acid, Chem. Commun. **46** (2010) 112. doi: https://doi.org/10.1039/B917705A
15. *Fernandez-Merino, M. J., Guardia, L., Paredes, J. I., Villar-Rodil, S., Solis-Fernandez, P., Martinez-Alonso, A., Tascón, J. M. D.*, Vitamin C is an ideal substitute for hydrazine in the reduction step of graphene oxide suspensions, J. Phys. Chem. C **114** (2010) 6426. doi: https://doi.org/10.1021/jp100603h
16. *Gao, J., Lui, F., Lui, Y., Ma, N., Wang, Z., Zhang, X.,* Environment-friendly method to produce graphene that employs vitamin C and amino acid, Chem. Mater. **22** (2010) 2213. doi: https://doi.org/10.1021/cm902635j
17. *Wang, Y., Shi, Z., Yin, Y.,* Facile synthesis of soluble graphene via a green reduction of graphene oxide in tea solution and its biocomposites, ACS Appl. Mater. Interfaces **3** (2011) 1127. doi: https://doi.org/10.1021/am1012613
18. *Zhu, C., Guo, S., Fang, Y., Dong, S.,* Reducing sugar: New functional molecules for the green synthesis of graphene nanosheets, ACS Nano **4** (2010) 2429. doi: https://doi.org/10.1021/nn1002387
19. *Khanra, P., Kuila, T., Kim, N. H., Bae, S. H., Yu, D. S., Lee, J. H.,* Simultaneous bio-functionalization and reduction of graphene oxide by baker's yeast, Chem. Eng. J. **183** (2012) 526. doi: https://doi.org/10.1016/j.cej.2011.12.075
20. *Dezhi, C., Lidong, L., Lin, G.,* An environment-friendly preparation of reduced graphene oxide nanosheets via amino acid, Nanotechnology **22** (2011) 325601. doi: https://doi.org/10.1088/0957-4484/22/32/325601
21. *Carrasco-Pancorbo, A., Cerretani, L., Bendini, A., Segura-Carretero, A., Del Carlo, M., Gallina-Toschi, T., Lercker, G., Compagnone, D., Fernández-Gutiérrez, A.,* Evaluation of the antioxidant capacity of individual phenolic compounds in virgin olive oil, J. Agric. Food Chem. **53** (2005) 8918. doi: https://doi.org/10.1021/jf0515680

22. *Kraljić Roković, M., Čubrić, M., Wittine, O.,* Phenolic compounds removal from mimosa tannin model water and olive mill wastewater by energy-efficient electrocoagulation process, J. Electrochem. Sci. **4** (2014) 215. doi: https://doi.org/10.5599/jese.2014.0066
23. *Baioun, A., Kellawi, H., Falah, A.,* A modified electrode by a facile green preparation of reduced graphene oxide utilizing olive leaves extract, Carbon Letters **24** (2017) 47. doi: https://doi.org/10.5714/CL.2017.24.047
24. *Sačer, D., Čapeta, D., Šrut Rakić, I., Peter, R., Petravić, M., Kraljić Roković, M.,* Tailoring polypyrrole supercapacitive properties by intercalation of graphene oxide within the layer, Electrochim. Acta **193** (2016) 311. doi: https://doi.org/10.1016/j.electacta.2016.02.055
25. *Enache, T. A., Amine, A., Brett, C. M. A., Oliveira-Brett, A. M.*, Virgin olive oil ortho-phenols—electroanalytical quantification, Talanta **105** (2013) 179. doi: https://doi.org/10.1016/j.talanta.2012.11.055
26. *Belaid, C., Khadraoui, M., Mseddi, S., Kallel, M., Elleuch, B., Fauvarque, J. F.*, Electrochemical treatment of olive mill wastewater: Treatment extent and effluent phenolic compounds monitoring using some uncommon analytical tools, J. Environ. Sci. **25** (2013) 220. doi: https://doi.org/10.1016/S1001-0742(12)60037-0
27. *Di Maio, I., Esposto, S., Taticchi, A., Selvaggi, R., Veneziani, G., Urbani, S., Servili, M.,* HPLC–ESI-MS investigation of tyrosol and hydroxytyrosol oxidation products in virgin olive oil, Food Chem. **125** (2011) 21. doi: https://doi.org/10.1016/j.foodchem.2010.08.025
28. *Tien, H. N., Luan, V. H., Cuong, T. V., Kong, B. S., Chung, J. S., Kim, E. J., Hur, S. H.,* Fast and simple reduction of graphene oxide in various organic solvents using microwave irradiation, J. Nanosci. Nanotechnol. **12** (2012) 5658. doi: https://doi.org/10.1166/jnn.2012.6340
29. *Eda, G., Lin, Y.-Y., Mattevi, C., Yamaguchi, H., Chen, H. A., Chen, S., Chen, C. W., Chhowalla, M.,* Blue photoluminescence from chemically derived graphene oxide, Adv. Mater. **22** (2010) 505. doi: https://doi.org/10.1002/adma.200901996
30. *Muthoosamy, K., Bai, R. G., Abubakar, I. B., Sudheer, S. M., Lim, H. N., Loh, W. S., Huang, N. M., Chia, C. H., Manickam, S.,* Exceedingly biocompatible and thin-layered reduced graphene oxide nanosheets using an eco-friendly mushroom extract strategy, Int. J. of Nanomed. **10** (2015) 1505. doi: https://doi.org/10.2147/IJN.S75213
31. *Hu, K., Xie, X., Szkopek, T., Cerruti, M.,* Understanding hydrothermally reduced graphene oxide hydrogels: From reaction products to hydrogel properties, Chem. Mater. **28** (2016) 1756. doi: https://doi.org/10.1021/acs.chemmater.5b04713
32. *Tang, B., Chen, H., Sun, S., Li, M., Wang, Z., Yu, H., Maa, T., Li, S.,* Influence from defects of three-dimensional graphene networks on the interface condition between the graphene basal plane and various resins, RSC Adv. **8** (2018) 27811. doi: https://doi.org/10.1039/C8RA04932G
33. *Fan, X., Peng, W., Li, Y., Li, X., Wang, S., Zhang, G., Zhang, F.,* Deoxygenation of exfoliated graphite oxide under alkaline conditions: A green route to graphene preparation, Adv. Mater. **20** (2008) 4490. doi: https://doi.org/10.1016/j.msec.2016.11.017
34. *Aouidia, F., Dupuy, N., Artaud, J., Roussos, S., Msallem, M., Perraud Gaime, I., Hamdi, M.,* Rapid quantitative determination of oleuropein in olive leaves (*Olea europaea*) using mid-infrared spectroscopy combined with chemometric analyses, Ind. Crops. Prod. **32** (2012) 292. doi: https://doi.org/10.3390/antiox4040682
35. *Zghari, B., Doumenq, P., Romane, A., Boukir, A.,* GC-MS, FTIR and 1H ,13C NMR structural analysis and identification of phenolic compounds in olive mill wastewater extracted from Oued Oussefrou effluent (Beni Mellal-Morocco), J. Mater. Environ. Sci. **8** (2017) 4496. doi: https://doi.org/10.26872/jmes.2017.8.12.475
36. *Solís-Fernández, P., Rozada, R., Paredes, J. I., Solís-Fernández, P., Rozada, R., Paredes, J. I., Villar-Rodil, S., Fernández-Merino, M. J., Guardia, L., Martínez-Alonso, A., Tascón, J. M. D.,* Chemical and microscopic analysis of graphene prepared by different reduction degrees of graphene oxide, J. Alloys Compd. **536** (2012) 532. doi: https://doi.org/10.1016/j.jallcom.2012.01.102
37. *Cheng, M., Yang, R., Zhang, L., Shi, Z., Yang, W., Wang, D., Xie, G., Shi, D., Zhang, G.,* Restoration of graphene from graphene oxide by defect repair, Carbon **50** (2012) 2581. doi: https://doi.org/10.1016/j.carbon.2012.02.016
38. *Araujo, P. T., Terrones, M., Dresselhaus, M. S.,* Defects and impurities in graphene- e materials, Mater. Today **15** (2012) 98. doi: https://doi.org/10.1016/S1369-7021(12)70045-7
39. *Chua, C. K., Ambrosi, A., Sofer, Z., Macková, A., Havránek, V., Tomandl, I., Pumera, M.,* Chemical preparation of graphene materials results in extensive unintentional doping with heteroatoms and metals, Chem. Eur. J. **20** (2014) 15760. doi: https://doi.org/10.1002/chem.201404205
40. *Martinez, S., Valek, L., Petrović, Ž., Petrović, Ž., Metikoš-Huković, M., Piljac Zegarac, J.,* Catechin antioxidant action at various pH studied by cyclic voltammetry and PM3 semi-empirical calculations, J. Electroanal Chem. **584** (2005) 92.
41. *Shin, H. J., Kim, K. K., Benayad, A., Yoon, S. M., Jin, M. H., Jeong, H. K., Kim, J. M., Choi, J. Y.,* Efficient reduction of graphite oxide by sodium borohydride and its effect on electrical conductance, Adv. Funct. Mater. **19** (2009) 1987. doi: https://doi.org/10.1002/adfm.200900167
42. *Wang, Y., Chen, Y., Lacey, S. D., Xu, L., Xie, H., Li T., Danner, V. A., Hu, L.,* Reduced graphene oxide film with record-high conductivity and mobility, Mater. Today **21** (2018) 186. doi: https://doi.org/ 10.1016/j.mattod.2017.10.008
43. *Ha, T., Kim, S. K., Choi, J.-W., Chang, H., Jang, H. D.*, Adv. Pow. Tech. **30** (2019) 18. doi: https://doi.org/10.1002/adma.201901924
44. *Hantel, M. M., Kaspar, T., Nesper, R., Wokaun, A., Kötz, R.,* Partially reduced graphene oxide paper: A thin film electrode for electrochemical capacitors, Journal of The Electrochem. Soc. **160** (2013) A747. doi: https://doi.org/10.1149/2.019306jes
45. *Oh, Y. J., Yooa, J. J., Kima, Y. I., Yoona, J. K., Yoona, H. N., Kima, J.-H., Park, S. B.*, Oxygen functional groups and electrochemical capacitive behavior of incompletely reduced graphene oxides as a thin-film electrode of supercapacitor, Electrochim. Acta **116** (2014) 118. doi: https://doi.org/10.1016/j.electacta.2013.11.040
46. *Zhang, W., Zhang, Y., Tian, Y., Yang, Z., Xiao, Q., Guo, X., Jing, L., Zhao, Y., Yan, Y., Feng, J., Sun, K.*, An insight into the capacitive properties of reduced graphene oxide, ACS Appl. Mater. Interfaces **64** (2014) 2248. doi: https://doi.org/10.1021/am4057562